A Comparative Analysis of Analytical Hierarchy Process and Fuzzy Logic Modeling in Flood Susceptibility Mapping in the Assaka Watershed, Morocco

Achraf Khaddari[1*], Abdessamad Jari[2], Saïd Chakiri[1], Hassan El Hadi[3], Allal Labriki[3], Soufiane Hajaj[2], Lahcen Goumghar[4], Abderrazak El Harti[2], Mohamed Abioui[5,6]

1 Laboratory of Geosciences, Department of Geology, Faculty of Sciences, Ibn Tofail University, 133, Kenitra, Morocco

2 Laboratory of Geomatic, Georesources and Environment, Faculty of Sciences and Techniques, Sultan Moulay Slimane University, 23000 Beni Mellal, Morocco

3 Geodynamics Laboratory of Old Chains, Department of Geology, Faculty of Sciences Ben M'Sik, Hassan II University, 7955 Casablanca, Morocco

4 Natural Resources and Sustainable Development Laboratory, Faculty of Sciences, Ibn Tofail University, Kenitra 133, Morocco

5 Geosciences, Environment and Geomatics Laboratory, Department of Earth Sciences, Faculty of Sciences, Ibnou Zohr University, Agadir 80000, Morocco

6 MARE-Marine and Environmental Sciences Centre, Sedimentary Geology Group, Department of Earth Sciences, Faculty of Sciences and Technology, University of Coimbra, Coimbra 3030-790, Portugal

* Corresponding author's e-mail: achraf.khaddari@uit.ac.ma

ABSTRACT

The Assaka watershed is one of the largest watersheds in the Guelmim region in southern Morocco. It is frequently exposed to the many flooding events that can be responsible for many costly human and material damages. This work illustrates a decision-making methodology based on Analytical Hierarchy Process (AHP) and Fuzzy Logic Modelling (FLM), in order to perform a useful flood susceptibility mapping in the study area. Seven decisive factors were introduced, namely, flow accumulation, distance to the hydrographic network, elevation, slope, LULC, lithology, and rainfall. The susceptibility maps were obtained after normalization and weighting using the AHP, while after Fuzzification as well as the application of fuzzy operators (OR, SUM, PRODUCT, AND, GAMMA 0.9) for the fuzzy logic methods. Thereafter, the flood susceptibility zones were distributed into five flood intensity classes with very high, high, medium, low, and, very low susceptibility. Then validated by field observations, an inventory of flood-prone sites identified by the Draa Oued Noun Hydraulic Watershed Agency (DONHBA) with 71 carefully selected flood-prone sites and GeoEye-1 satellite images. The assessment of the mapping results using the ROC curve shows that the best results are derived from applying the fuzzy SUM (AUC = 0.901) and fuzzy OR (AUC = 0.896) operators. On the other hand, the AHP method (AUC = 0.893) shows considerable mapping results. Then, a comparison of the two methods of SUM fuzzy logic and AHP allowed considering the two techniques as complementary to each other. They can accurately model the flood susceptibility of the Assaka watershed. Specifically, this area is characterized by a high to very high risk of flooding, which was estimated at 67% and 30% of the total study area coverage using the fuzzy logic (SUM operator) and the AHP methods, respectively. Highly susceptible flood areas require immediate action in terms of planning, development, and land use management to avoid any dramatic disaster.

Keywords: Assaka watershed; flood susceptibility; GIS; multi-criteria analysis; FLM, AHP.

INTRODUCTION

The risk of flooding is one of the most frequent and damaging natural disasters. It threatens several regions around the world (Tanguy, 2012). It is mainly related to several factors as climate changes, population growth, and abusive land use. Indeed, floods constitute 31% of all the resulting

damage from natural disasters, and more than 90 countries with approximately 196 million persons are exposed to catastrophic floods (Zorn, 2018). Morocco is among the countries that show a high vulnerability to natural hazards, and 70% of these events are flooding. In the last decades, this type of disaster has affected more regions and become a real increasing threat, due to the growing occupation of vulnerable areas following climate change on the other, then generating strong localized storms causing rapid and violent floods. In this frame, over the past two decades, 20 major events have been recorded in Morocco with an estimated average cost of 450 million US$ per year (Echogdali et al., 2018; Karmaoui et al., 2014). Floods generally occur following a heavy rainfall of a long duration or snowmelt and are capable of transforming dry wadi beds into violent and destructive torrents. On the timescale, the most important flood events in Morocco were revealed in the Ourika valley (1995), the Martil plain (2000), Berrechid and Settat regions (2002), the Tan-Tan, Nador, Al Hoceima, and Khenifra regions, the Tangiers region (2008), the Gharb plain (2003), the Taza region (2010) and the Guelmim region (2014)(Argaz et al., 2019).

The Wadi Assaka watershed, located in the Guelmim-Oued Noun region (southern Morocco), is one of the most flooded regions in Morocco. However, the most severe floods in this watershed were recorded in 1968, 1985, 2010, and 2014. Latter these led to catastrophic and exceptional flooding in the region's rivers, especially the Wadi Sayyed and the Wadi Oum Laâchar, which are the main tributaries of the Oued Assaka (Talha et al., 2019). This region experienced during the period from 11/20/2014 to 12/01/2014 exceptional rainfall which reached 260 mm in the city of Guelmim, with a very high intensity that exceeded 200 mm for 12 hours, which generated exceptional floods in the watershed of Assaka (El Mahmouhi et al., 2016; Mirari & Benmlih, 2018; Theilen-Willige et al., 2015). In the last decades, this watershed is currently experiencing a high and accentuated demographic evolution, with uncontrolled land use, which makes the population and property very vulnerable to violent floods. As a result, 47 people lost their lives in the provinces of Sidi Ifni and Guelmim regions. In parallel, the damage was estimated at more than USD 600 million. Road cuts, dykes breaches, and power cuts have been caused and affected a large part of the populated zones (AIDE et al., 2015; Talha et

al., 2019). This requires a well-defined flood risk reduction strategy to propose measures to protect people and property at risk.

In this context, vulnerability reduction is essentially based on the assessment and prediction of flood risks. This is an essential step for appropriate land use planning in flood-prone areas. Several approaches (Geographic Information Systems, remote sensing, and hydraulic models) have been used to accurately assess areas of flooding high vulnerability (Demir & Kisi, 2016; Farhadi & Najafzadeh, 2021; Siahkamari et al., 2018). So far, hydrological and hydraulic modeling remains the most efficient techniques, allowing a more accurate estimation of depth, flow velocity, and flood extent for different return periods (Msaddek et al., 2020; Nguyen et al., 2016). However, the use of these modeling methods requires a high-resolution terrain elevation model. Thus, very high rainfall and hydrographic measurements, are not continuously available (Komi et al., 2017; Werren et al., 2016). In recent years, researchers have developed alternative techniques for the assessment of short-duration, high-intensity, multi-scale floods, combining the factors conditioning the occurrence of these natural hazards (Ha et al., 2023; Mudashiru et al., 2021; Ongdas et al., 2020). In light of geographic information systems and space technology, several multi-criteria decision analysis models and high-performance indices are widely used. Such as frequency ratio (Samanta et al., 2018), logistic regression (Shafapour Tehrany et al., 2019), statistical index model (Khosravi et al., 2016), entropy index (Malekinezhad et al., 2021), flood risk index (FHI) (Ikirri et al., 2022), artificial neural network (Wang et al., 2020), analytic hierarchy process (Hammami et al., 2019), fuzzy logic models (Sahana & Patel, 2019). AHP and FLM are widely applied in several parts of the world. They have also been approved as simple and robust methodologies for decision-making in water resources management, floods, landslides, and forest fires (Bouamrane et al., 2022; Li et al., 2018; Pourghasemi et al., 2016; Vakhshoori & Zare, 2016). In particular, when the two methods' performances were compared, FLM demonstrates better results (Bouamrane et al., 2022; Mohamed & Elmahdy, 2017).

In the Assaka watershed, it is important to note that no previous studies have been undertaken for flood susceptibility, neither using the AHP nor using the FLM. However, several other studies in several regions of the world have mentioned that

both techniques (AHP, fuzzy logic) were able to provide more reliable results for flood hazard susceptibility mapping (Hammami et al., 2019; Mudashiru et al., 2021; Sahana & Patel, 2019). The objective of the present research is to introduce an integrated approach that will allow the testing and analyze several fuzzy logic models and AHP, separately in a GIS environment. Furthermore, the result of our study will be a practical solution for flood susceptibility mapping in the Assaka watershed.

MATERIALS AND METHODS

Study area geographical and geological setting

The Wadi Assaka watershed, the subject of this study, is located in southern Morocco in the Guelmim-Oued Noun region. This area is a hydraulic sub-watershed of Guelmim, it occupies an area of 6866 km², corresponding to a perimeter of 750 km, with a total population of more than 18780873 according to the 2014 census (MIRARI, 2022). It is constituted by a network of Wadis (tributaries) along which there are several floodwater spreading areas. The hydrographic network is composed of 3 sub-catchments of the main Wadis namely, Oued Sayyed, Oued Ouerguennoun, and Oued Oum Al Achar (Bannari et al., 2018). Geographically, the Assaka watershed is located between the two parallels 28.54° and 29.47° N, and the two meridians 10.42°, and 9.02° W (Figure 1).

From a geomorphological and geological point of view, the Assaka catchment area is located between the depressions of the Guelmim-Bouizakarne plain to the north, the valley of the Oued Seyyad-Ouerguennoun in the center and the northern flank of the Jbel Guir-Taïssa in the south-west. The mountain ranges are in the form of a complex syncline surrounded to the north, west, and south by three anticlinal buttonholes which are Kerdous, Ifni, and Jbel Guir (ATBIR et al.; Bannari et al., 2018; Mathieu et al., 2004; Soulaimani & Bouabdelli, 2005). Indeed, the altitudes vary from 0 m on the coasts and the plain to 1483 m at the extreme North-East of the watershed, and the average altitude is around 650 m. Geologically, the previous studies on the study area revealed lithological formation's preferential orientation with a NE-SW trend. The formations present a synclinal structure and demonstrate ages from the Precambrian to the Quaternary. All the terrain constituting the height altitudes are Precambrian or Cambro-Silurian, and consist of the litho-units of quartzite, limestone, and shale which appear in the center of the plain at the level of Jbel Tayert; whereas the plain is generally constituted by deposits of Plio-Quaternary cover overlying the Acadian
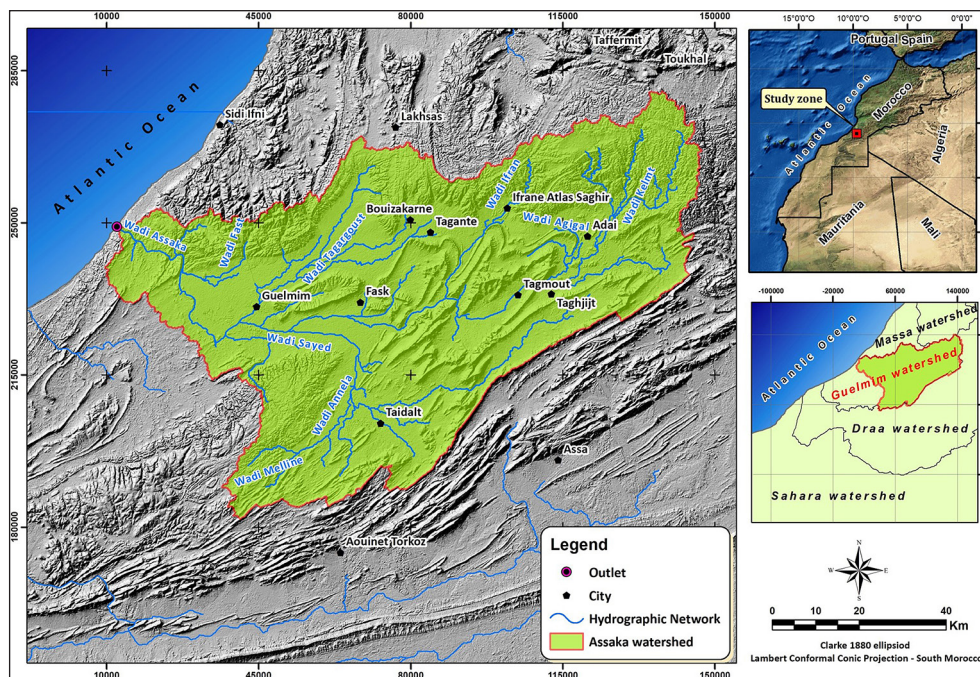

Figure 1. Location map of the Assaka watershed

shales of the substratum (El Mahmouhi et al., 2016; Soulaimani & Ouanaimi, 2011).

The climatology of the area is characterized by severe aridity due to the presence of the High Atlasic belt, which prevents rainy disturbances from the north toward the south (El Mahmouhi et al., 2016). The average annual rainfall is around 115 mm in Guelmim, with a very important random irregularity, between 90 mm and 160 mm at the watershed level. This fluctuation in the rainfall regime over the years is the cause of increased flooding in the watershed (Amouch et al., 2020; Talha et al., 2019). When the average annual temperature is around 21 °C in Guelmim.

Flood mapping methodology

As mentioned earlier, the approach adopted in this study is based on the integration of multi-criteria decision analysis, GIS, and spatial remote sensing. The overall methodology is presented in the flow chart (Figure 2). This analysis involved seven flood susceptibility conditioning factors, namely flow accumulation, altitude, slope, land use, distance to the river, lithology, and precipitation. These factors were selected based on a literature review, expert opinions, and their relevance in several case studies in other Moroccan regions (Echogdali et al., 2022; El Morjani et al., 2016; Ikirri et al., 2022; Talha et al., 2019). The different thematic layers related to these factors were generated in a GIS environment. Then, all the extracted maps were combined according to the importance of each factor, using two methods in the order to assess their capability in flood susceptibility mapping within the Assaka watershed: (1) the Analytical Hierarchy Process (AHP), which requires the standardization of the causal factors, the using a pairwise comparison matrix between the factors' evaluations, thus obtaining a weight for each criterion. Afterward, to ensure the accuracy of the standardization and weighting, the consistency ratio (CR) is calculated to examine the results of the determination stage. Once the evaluation criteria layers have been established, it remains to combine the thematic maps, using a mathematical aggregation formulation in a GIS environment, to finally obtain a susceptibility map; (2) Fuzzy Logic methods that were carried out in two-step steps, namely the fuzzy membership and fuzzy gamma overlay functions in ArcMap10.5. A LINEAR Fuzzy membership function was performed on all the conditioning factors. Thus, the data fuzzification and conversion were established, where the zero and one values reflect the level of certainty of the used members. The flood factors were combined using various fuzzy operators, including AND, OR, SUM, PRODUCT, and GAMMA, allowing the production of several flood susceptibility maps. Finally, the set of flood susceptibility maps created by each model according to the AHP and fuzzy operators will be tested and compared using the Receiver Operating Characteristic (ROC)
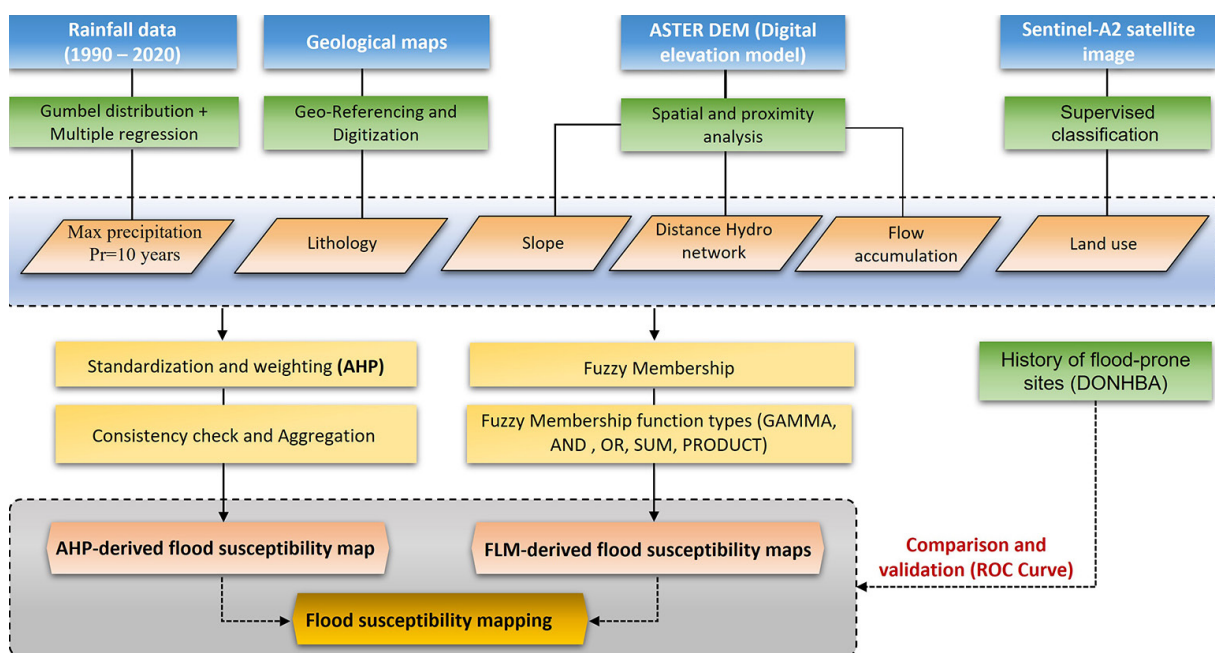

Figure 2. Flowchart of the methodology adopted to generate the flood susceptibility map

Table 1. Data used for flood susceptibility mapping

Data type	Resolution	Year	Source
ASTER-DEM Digital Elevation Model (DEM)	30 m	2009	https://earthexplorer.usgs.gov
Slope	30 m	2009	Derived from DTM (Aster- DEM)
Flow accumulation	30 m	2009	Derived from DTM (Aster- DEM)
Hydrographic network	30 m	2009	Derived from DTM (Aster- DEM)
Sentinel-2A	VNIR 10 m	2020	https://earthexplorer.usgs.gov
Land use	10 m	2020	Derived from Sentinel-2 VNIR bands
Lithology	30 m	1951	Digitized from the geological map ofGuelmim and Draa-lower at a scale of 1:200,000
Precipitation	30 m	1990–2020	Multiple climate stations and regression modeling
Flood sites	Shapefile (points)	2006–2020	Draa-Oued Noun Hydraulic Watershed Agency (DONHBA)

curve and Area Under the Curve (AUC) in Arc-GIS 10.5 software.

These methods have several advantages. Firstly, they provide realistic estimates without the use of empirical models as well as they are based only on historical data on flooding distribution and causal factors (Bouamrane et al., 2022; El Morjani et al., 2016). Secondly, these techniques take into account both the susceptibility of each area to flooding and factors related to flooding emergency management. Thirdly, this input also results in a considerable gain of time and therefore a cost reduction. The data required for the application of the methodology were collected from various sources (Table 1). The processing of these data allowed to elaborate of a useful spatial dataset to perform this study, following a multi-criteria analysis.

Preparation and analysis of causal factors

Elevation

The probability of occurrence of flood events is inversely proportional to altitudes, therefore flat areas at low altitudes are most affected by the risk of flooding, making it a reliable indicator of susceptibility to flood events (Hammami et al., 2019; Wang et al., 2018). The elevation data used in our study is derived from ASTER data (ASTER GDEM) available on the website (https://earthexplorer.usgs.gov). The ASTER GDEM has a spatial resolution of 30 m. For our study, 6 Scenes were downloaded, processed, and geo-referenced according to Lambert's conformal conical projection system – southern Morocco, then we automatically delineated the watershed of Assaka and the result was validated by the

Guelmim, Fask, Sidi Ifni, Bouizakarn, Tarhjijt, and Assa1: 100,000 topographic maps. The Assaka watershed has a very varied topography, ranging from 0m on the coast and plain to 1483m in the extreme northeast where the mountain ranges from a complex syncline (Figure 3a).

Slope

The slope is a factor that affects the runoff and the infiltration of surface water. Low slope areas are those that contribute to the infiltration of water into the soil, therefore leading to a higher flood hazard susceptibility and vice versa (Costache et al., 2019; Ikirri et al., 2022; Shafapour Tehrany et al., 2019). Obviously, in our study area, the high-slope areas are the mountainous regions (upstream), while the low-slope areas are concentrated downstream (plain) towards the outlet of the Wadi Assaka. The slope map was created from the elevation data and has slope ranges varying between 0 and >30, using the spatial analyst tool integrated in ArcGIS 10.5 software (Figure 3b).

Flow accumulation

Areas that are close to the flow accumulation path and particularly where a large volume has accumulated upstream are more susceptible to flooding events (Dash & Sar, 2020; Ikirri et al., 2022; Vignesh et al., 2021). The flow accumulation factor is derived from the DEM as a cumulative weight of all flowing cells in each downslope cell of the output raster. Cells with high flow accumulation are areas of concentrated flow that can be used to identify flow channels. Cells with zero flow accumulation presenting local high topographic areas can be used to identify topographic ridges or peaks. Then, the resulting
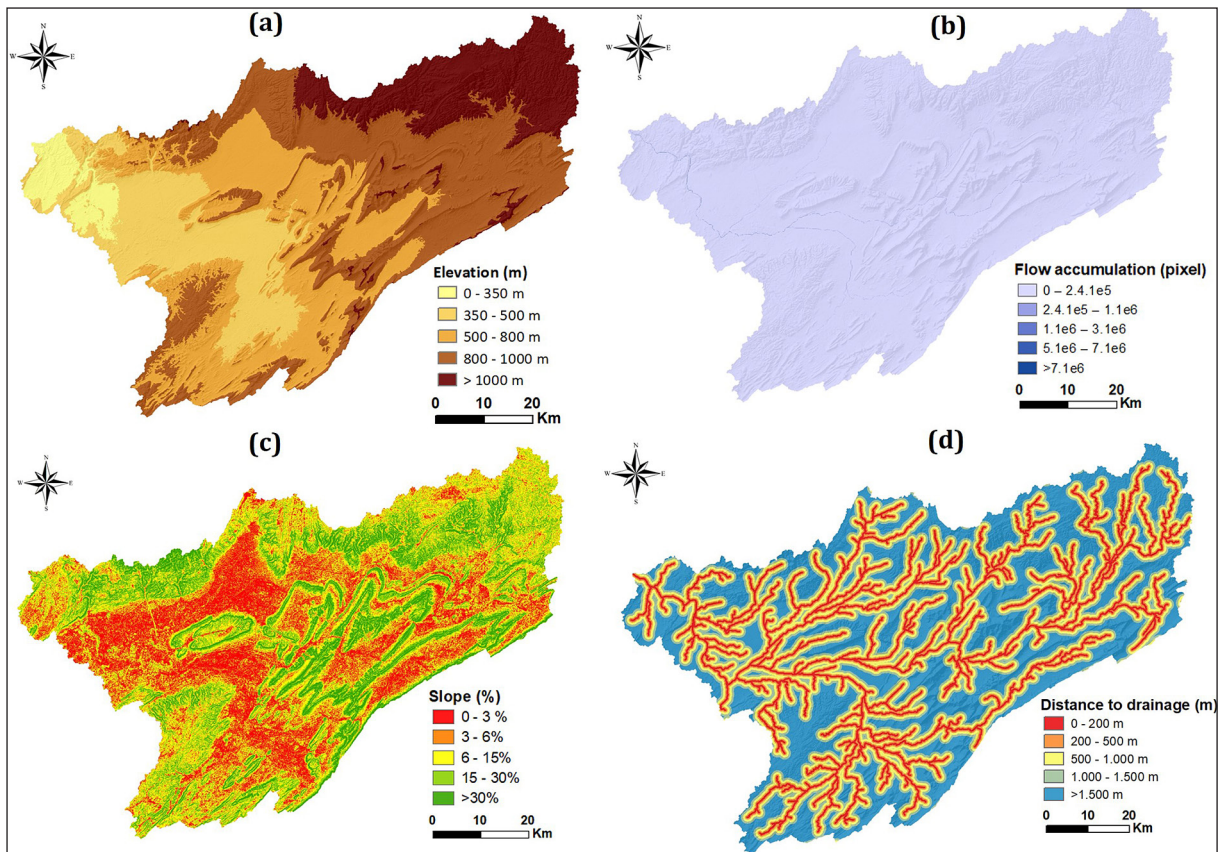
Figure 3. (a) Elevation map; (b) slope map; (c) flow accumulation map;
(d) map of distance from the hydrographic network

map is classified into five levels according to the volume of accumulated water. The highest value corresponds to the lowest areas of our watershed (Figure 3c).

Distance from the hydrographic network

River overflows are crucial for triggering a flood. This is why the distance from the rivers is one of the main factors in flood susceptibility studies [22, 47]. The effect of the wadi bed decreases when the distance increases. This explains why the distance from the hydrographic network will have to constitute a high weight in our final decision. The classes of this factor have been defined by processing the historical flood records in the study area. Globally, a distance between 0 and 200 m presents a very high flood risk zone, while the effect of this parameter becomes weak from 1500 meters to the drainage network. The map of this factor was generated from the DEM, by estimating the hydrographic network from the flow accumulation layer, adopting the most adequate accumulation threshold to reproduce the hydrologic networks. In our case, after testing many thresholds, a

value of 8,000 cells (or more) was retained. Next, five different buffer zones were generated, applying the Euclidean distance (Figure 3d).

Land use

Land use directly or/and indirectly controls flood susceptibility, by influencing anthropogenic practices such as urbanization and agricultural use. The latter allows the impermeable areas growth. Most of these areas showed a high correlation with the appearance of flooding areas (Apollonio et al., 2016; Barkey et al., 2020; El Morjani et al., 2016). In the present study, the land cover map was generated using the Sentinel-2Adata, which has a high spatial resolution (10 m) than other medium spatial resolution images (Çavur et al., 2019; Phiri et al., 2020).

Thereafter, the pre-processing and the classification supervised by the maximum likelihood algorithm, we were able to obtain nine classes, namely: agriculture, forest, built-up area, light bare soil, dark bare soil, light-colored rocky terrain, dark colored rocky terrain, alluvium, sparse vegetation (Figure 4a). These results

were validated using high spatial resolution images (GeoEye-1) and field missions; thus Cohen's Kappa statistical coefficient (K) judged a value of 88.3%, which remains satisfactory in our study. Then, this map will be classified as follows:

- The highest values correspond to impermeable areas or plains (built-up areas, alluvial areas) which promote the quick water flow and subsequently the occurrence of floods;
- The lower values represent the infiltration zones (vegetation, forest);
- The other classes were assigned to intermediate values.

Lithology

The lithology is an important factor in the genesis of floods. Generally, surface geology has different degrees of permeability, which control the water infiltration rate (Costache et al., 2019; Morjani, 2011). The lithological distribution map of the Assaka watershed was developed using the assembly of the two 1: 200,000geological maps of Guelmim -Draa-lower and Foum Elhassane-Assa, in the western Anti-Atlasic belt. The resulting lithological map was classified according to the rock permeability. The classification distinguishes the more permeable areas by the lower values and vice versa (Figure 4b).

The analysis of this map showed that the study area is mainly made up of shales, limestones, sandstones, and quartzites lithological units, that present various geological ages, from the Precambrian to the Quaternary (Mathieu et al., 2004; Soulaimani & Ouanaimi, 2011).

Precipitation

Precipitation intensity is a very important climatic factor that contributes to the susceptibility of an area to be flooded (El Morjani et al., 2016; Hammami et al., 2019). The magnitude of flooding increases proportionally with the amount of rain and snowfall at a given location. Estimating and mapping extreme precipitation is an essential step in a flood susceptibility study, especially at the scale of a large watershed where climatological variables experience spatiotemporal changes (El Morjani, 2002; Marengo et al., 2021; Tabari, 2020). In this study, we used the annual maximum total precipitation on 4 consecutive days, to elaborate a maximum precipitation map for a return period of 10 years, which will allow a better evaluation of the flood

susceptibility (Kouassi et al., 2018; Morjani, 2011). The realization of this map goes through the following steps:

- Step 1: Statistical analysis of rainfall data and estimation of missing measurements, using daily rainfall data for the period 1990-2020 was extracted from 8 meteorological stations located around the Assaka watershed. These data were retrieved from the Draa Oued Noun Hydraulic Watershed Agency (DONHBA);
- Step 2: Calculation and statistical analysis of the series of maximum daily precipitation over four days for a return period of ten years using the distribution function of the Gumbel law (Andrade et al., 2015; Gumbel, 1957; Onen & Bagatur, 2017; Tie et al., 2007);
- Step 3: Choice of the spatial interpolation method to obtain the maximum daily precipitation map corresponding to a 10-year return period (Chen & Liu, 2012; Grillakis et al., 2020). In the order to perform the study area precipitation map, we used multiple linear regressions, which show very satisfactory results in terms of rainfall mapping. This method takes into account the factors influencing the spatial distribution of rainfall (elevation, longitude, latitude, distance from the ocean, exposure, and slope) that are responsible for the precipitation spatial variation (El Morjani, 2002; Goovaerts, 2000; Hu et al., 2019; Khaddari et al., 2022; Odabas et al., 2014). This technique describes the relationship between the dependent or explained variable (water levels) and a set of explanatory variables (station altitude, longitude, latitude, and proximity to the Atlantic Ocean). The selected model confirmed that almost 94.4% (R^2 = 0.9439) of the variation in rainfall is explained by the three explanatory variables retained in the regression equation. This is satisfactory, as the proportion that remains unexplained (5.6%). Furthermore, the value of the RMSE (2.2489) is low, indicating the performance of the model. The Fisher test (F) is used, as the probability associated with the F, in this case, is less than 0.0005, which means that we take a risk of error of less than 0.05% in concluding that the explanatory variables provide a significant amount of information to the model. The result of this analysis is a distribution map of the maximum annual rainfall on 4 consecutive days for a 10-year return period (Figure 4c).
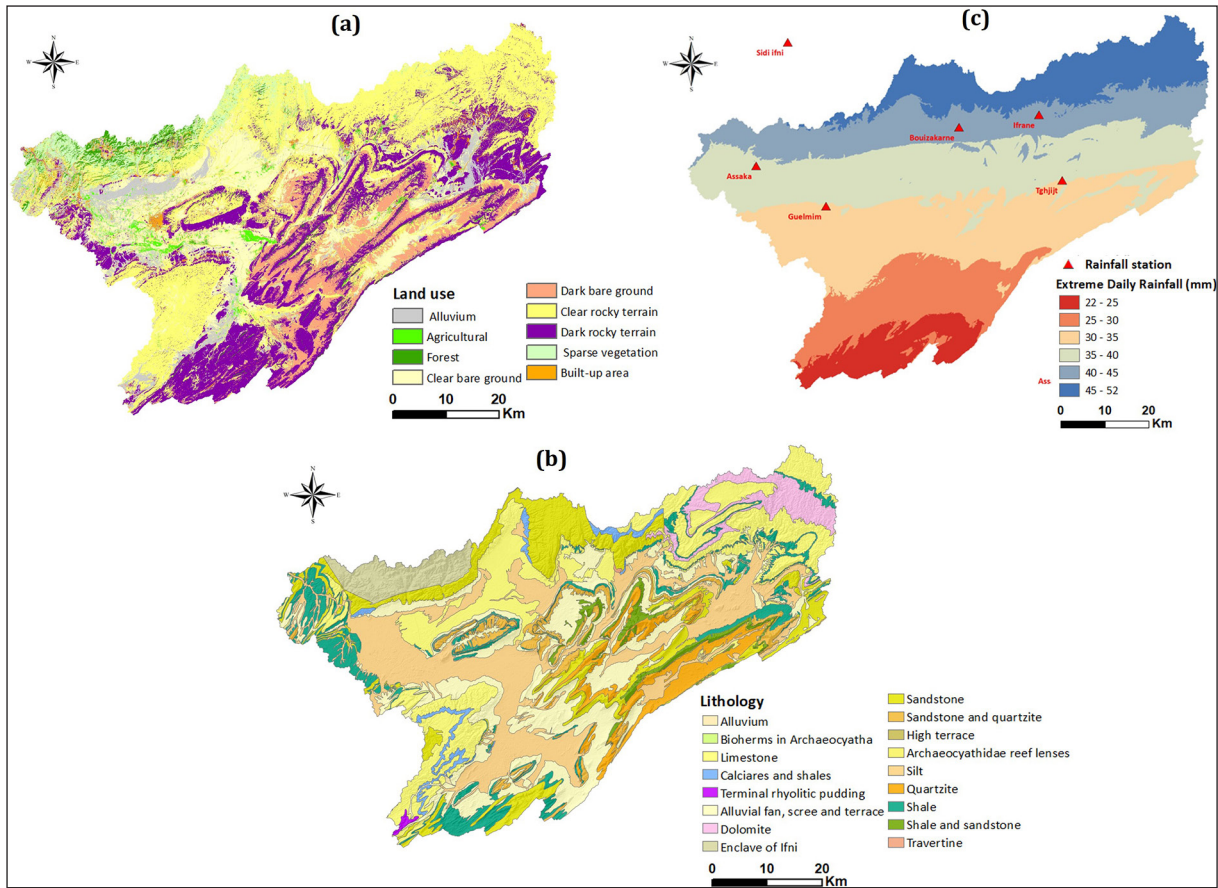
Figure 4. (a) Land use map; (b) lithological map; (c) map of maximum
4-day total precipitation for a 10-year return period

Analytical hierarchy process (AHP)

The objective of this study on flood risk mapping cannot be achieved if it depends on a single function (a single criterion) because "reality" is multidimensional, so it is natural to take into account several points of view to help in the decision (El Morjani, 2002). In this sense, the AHP is used primarily as a semi-qualitative approach to decision-making. It consists in performing a weighting based on a pairwise matrix comparison of causal factors (Saaty, 1990; Wang et al., 2018). This approach has been widely applied for flood risk mapping. It is considered to be a flexible and robust technique, as it allows for the adjustment of criterion priorities by improving the decision-making process (d'Avignon & Sauvageau, 1996; El Morjani, 2002; Jari et al., 2022; Roy & Bouyssou, 1993; Saaty, 1990; Wang et al., 2018). In the methodology of this research, the application of the AHP goes through the following steps: (1) Standardization and weighting of assessment criteria; (2) Consistency check; (3) Aggregation of criteria.

Standardization and weighting of assessment criteria

Once all the flood susceptibility causality criteria (the commonly used are Flow accumulation, Distance from the hydrographic network, Elevation, LULC, precipitation, slope and lithology) have been determined hierarchically (El Morjani, 2002; Hammami et al., 2019; Morjani, 2011; Yurdakul, 2004), a pairwise comparison matrix was created for each factor to allow a concrete assessment of the relative importance of each parameter. This comparison of the relative importance between criteria was rated from 1 to 9, indicating the less important to the much more important criteria, respectively (Table 2).

Our methodology consists of a hierarchical pairwise comparison using a 7×7 matrix, where the diagonal elements are equal to 1 (Table 3). The values of each row are compared to those of each column to define the relative importance and obtain the evaluation score. As an illustration, flow accumulation is a strongly more important parameter than land cover, in this case, it should be assigned the value of 5. The

Table 2. Verbal and numerical expression of the relative importance of a pair of criteria

Verbal expression of the relative importance of one criterion compared to another	Numerical
Equally important	1
Weakly important	3
Moderately important	5
Very important	7
Extremely important	9
Less important	1/2
Much less important	1/5
Very Much less important	1/7
Extremely less important	1/9

line describes the importance of the occupation. Therefore, the line represents the inverse value of the pairwise comparison (e.g., 1/5 for flux accumulation). Then, we will calculate the normalized index by dividing the total rate by the individual rate (Table 3). Based on the individual importance, a total weight (W) of 1 was assigned, after dividing among the seven parameters (Table 4).

Consistency check

The consistency ratio CR is considered a mathematical indicator of the judgment of a random decision (Saaty, 1977, 1990; Saaty & Vargas, 2012). A coherent judgment of the comparisons is made, the value of CR must be strictly lower than 0.1, otherwise, the coefficients of the comparison matrix are inconsistent. Then, in the order to evaluate the consistency level of our analytic hierarchy process matrix, the CR was used following (Eq. 1):

$$CR = \frac{CI}{RI} \qquad (1)$$

where: CR – consistency ratio;
CI – consistency index;
RI – randomized index.

Table 5 shows the values of the randomized index (RI). These values depend on the number of factors chosen (Saaty & Vargas, 2012; Yurdakul, 2004). In our study, the number of factors is equal to seven, and therefore the RI = 1.32.

Table 3. Pairwise comparison matrix of flood causality parameters. F_acc: flow accumulation, D_HN: Distance from the hydrographic network, Pdmax_10 yrs: Annual maximum total precipitations for a 10-year return period

Parameter	F_acc	D_HN	Altitude	Land use	Pdmax_10 yrs	Slope	Lithology
F_acc	1	2	2	5	5	5	7
D_HN	1/2	1	3	3	3	4	6
Altitude	1/2	1/3	1	3	3	3	6
Land use	1/5	1/3	1/3	1	2	2	3
Pdmax_10 yrs	1/5	1/3	1/3	1/2	1	2	3
Slope	1/5	1/4	1/3	1/2	1/2	1	4
Lithology	1/7	1/6	1/6	1/3	1/3	1/4	1

Table 4. Standardized flood susceptibility parameters for the hierarchical analysis process. Wi – weigh

Parameter	F_acc	D_HN	Altitude	Land use	Pdmax_10 yrs	Slope	Lithology	Wi
F_acc	0.36	0.45	0.28	0.38	0.34	0.29	0.23	0.33
D_HN	0.18	0.23	0.42	0.23	0.20	0.23	0.20	0.24
Altitude	0.18	0.08	0.14	0.23	0.20	0.17	0.20	0.17
Land use	0.07	0.08	0.05	0.08	0.13	0.12	0.10	0.09
Pdmax_10 yrs	0.07	0.08	0.05	0.04	0.07	0.12	0.10	0.07
Slope	0.07	0.06	0.05	0.04	0.03	0.06	0.13	0.06
Lithology	0.05	0.04	0.02	0.03	0.02	0.01	0.03	0.03

Table 5. Values of the randomized index used to calculate the consistency ratio

Number of criteria (n)	1	2	3	4	5	6	7	8	9	10
Randomized index (RI)	0	0	0.58	0.90	1.12	1.24	1.32	1.41	1.45	1.49

Table 6. Classes and weights of flood susceptibility decision factors using AHP

Causal factors	Class	Intensity	Rating	Weight
Flow accumulation (pixel)	> 7.106	Very high	10	0.33
	5.106–7.106	High	8	
	1.106–3.106	Medium	6	
	2,4.105–1.106	Low	4	
	0–2,4.105	Very low	2	
Distance from the hydrographic network (m)	0- 200	Very high	10	0.24
	200–500	High	8	
	500–1000	Medium	6	
	1000–1500	Low	4	
	> 1500	Very low	2	
Elevation (m)	0–350	Very high	10	0.17
	350–500	High	8	
	500–800	Medium	6	
	800–1000	Low	4	
	> 1000	Very low	2	
Land use	Alluvium and built-up area	Very high	10	0.1
	Agriculture	High	8	
	Bare soil and rocky terrain	Medium	6	
	Sparse vegetation	Low	4	
	Forest	Very low	2	
Maximum precipitation (mm)	> 45	Very high	10	0.07
	35–45	High	8	
	30–35	Medium	6	
	25–30	Low	4	
	< 25	Very low	2	
Slope (%)	0–3	Very high	10	0.06
	3–6	High	8	
	6–15	Medium	6	
	15–30	Low	4	
	> 30	Very low	2	
Lithology	Sandstone and massive quartzite	Very high	10	0.03
	Limestone, siltstone, dolomite, shale, and sandstone with clay intercalation	High	8	
	Tuffs, alluvial cone, fractured limestones, and shales	Medium	6	
	Terrace, old alluvial cone, scree, lacustrine limestone	Low	4	
	Alluvium et recent Reg	Very low	2	

The consistency index can be calculated using (Eq. 2):

$$I = \frac{\lambda_{max} - n}{n - 1} \qquad (2)$$

where: λ_{max} – maximum proper value;
　　　n – number of criteria.

In our study, the CI was calculated for λ_{max} = 7.35, n = 7, and RI = 1.32. Finally, the consistency ratio was calculated as CR = 0.04. This value is strictly below the threshold (0.1), which means an acceptable consistency of the pairwise comparison matrix.

Aggregation of criteria

Once the assessment criteria layers have been established and assigned to weighting coefficients (Table 6), it only remains to combine

these information planes using a mathematical formulation of a priori aggregation of criteria into a single criterion (Eq. 3). The weighted overlay of factors in raster format is performed using the raster calculator in ArcGIS 10.5.

$$A = \sum_{i=1}^{n} P_i V_i \qquad (3)$$

where: A – aggregation of criteria;
P_i – weight of criterion I;
V_i – standardized value of the factor i criterion;
n – number of criteria i.

Applying this mathematical formula, we obtain the following result (Eq. 4)

$$A = (0.33 \times FlowAcc) + (0.24 \times D_{RH}) + \\ +(0.17 \times Elevation) + (0.1 \times Landuse) + \\ +(0.07 \times Precip_{max}) + (0.06 \times Slope) + \\ +(0,03 \times Lithology) \qquad (4)$$

Fuzzy logic modeling (FLM)

FLM in a GIS environment is a successful knowledge-based method, highly adopted in several research fields (Hajaj et al., 2023; Nwazelibe et al., 2023; Schwarz & Kuleshov, 2022). It has also allowed, a multifactor analysis to estimate the flood susceptibility in several areas around the world in a semi-qualitative way (Akay, 2021; Sahana & Patel, 2019; Vakhshoori & Zare, 2016). Floods are considered to be hazards for which no suitable large-scale quantitative probabilistic model exists. However, the fuzzy logic system allows for modeling cause and effect relationships, assessing the degree of risk exposure, and consistently ranking the main conditioning criteria, taking into account available data and expert opinions (Tah & Carr, 2000). This approach also involves standardizing factors based on a series of mathematical formulae, which allow the modeling of imprecision and uncertainty in complex scientific problems (Parsian et al., 2021; Zadeh, 1965).

Factors standardization with fuzzy membership function

In practice, fuzzy logic consists of standardizing or reclassifying raw input data into a normalized scale, using a transformation function judged by experts. Member values can take any value between 0 and 1, reflecting the

degree of certainty of those members (Nandalal & Ratnayake, 2011; Sonmez & Bizimana, 2020). Values closer to 1 are the most suitable for the expected purpose (full membership), while those closer to 0 are the least suitable (no membership). Indeed, fuzzy membership functions are numerous. In studies related to spatial flood susceptibility mapping, sets of input values are converted to fuzzy values using a linear fuzzy membership function (Sahana & Patel, 2019; Siler & Ying, 1989). This function is presented as follows:

$$\mu(x) = 0 \; if \; x < min, \mu(x) \\ \mu(x) = 1 \; if \; x > max, \mu(x) \\ Otherwise \; \mu(x) = \frac{(x - min)}{(max - min)} \qquad (5)$$

This function defines a linear relationship with the minimum and maximum values. If the values are lower than the minimum value, 0 is assigned, while if the values are higher than the maximum value, 1 is assigned. This function is used to establish the fuzzification. For each factor, a membership function is determined, and then, based on the experts' knowledge, these criteria can be normalized (Table 7).

Fuzzy overlay

The application of fuzzy operators allows the generation of flood susceptibility maps. For this purpose, the five main operators were used in the fuzzy inference network (Sadeghi & Khalajmasoumi, 2015; Siler & Ying, 1989; Vakhshoori & Zare, 2016).

- Fuzzy OR (Eq. 6) – this operation allows the extraction of a maximum degree of membership and maximum uses. Indeed, between two membership functions, this operation chooses the maximum value.

$$\mu(x) = max\{\mu_1(x), \mu_2(x), \dots, \mu_n(x)\} \qquad (6)$$

where: μ_1, μ_2 et, μ_n – represent the values of the membership pixels in a raster;
n – the number of membership pixels in the concerned raster.

- Fuzzy AND (Eq. 7) – this operation allows intersection which extracts the minimum degree of membership. It uses the minimum pixel value of all the rasters to generate the susceptibility map.

$$\mu(x) = min\{\mu_1(x), \mu_2(x), \dots, \mu_n(x)\} \qquad (7)$$

Table 7. Fuzzification of factors using fuzzy logic methods

Causal factors	Class	Fuzzy membership value
Flow accumulation (pixel)	>7.106	1
	5.106–7.106	0.8
	1.106–3.106	0.5
	2,4.105–1.106	0.2
	0–2,4.105	0
Distance from the hydrographic network (m)	0–200	1
	200–500	0.75
	500–1000	0.5
	1000–1500	0.25
	> 1500	0
Elevation (m)	0–350	1
	350–500	0.85
	500–800	0.64
	800–1000	0.3
	> 1000	0
Land use	Alluvium and built-up area	1
	Agriculture	0.8
	Bare soil and rocky terrain	0.48
	Sparse vegetation	0.32
	Forest	0
Maximum precipitation (mm)	> 45	1
	35–45	0.63
	30–35	0.42
	25–30	0.2
	< 25	0
Slope (%)	0–3	1
	3–6	0.86
	6–15	0.54
	15–30	0.17
	>30	0
Lithology	Sandstone and massive quartzite	1
	Limestone, siltstone, dolomite, shale, and sandstone with clay intercalation	0.73
	Tuffs, alluvial cone, fractured limestones, and shales	0.56
	Terrace, old alluvial cone, scree, lacustrine limestone	0.27
	Alluvium et recent Reg	0

• Fuzzy RODUCT (Eq. 8) – this operation consists of the multiplication of the membership functions. The result in this case will be a small value of less than 1. In general, the pixel values in the final raster tend to be zero.

$$\mu(x) = \prod_{i=1}^{i=n} \mu_i \qquad (8)$$

where: μ_i is the membership value of the pixels in factor i.

• Fuzzy SUM (Eq. 9) – in contrast to the Fuzzy PRODUCT function, this operation consists of linearly combining the membership functions, so that the final raster contains pixel values that tend towards 1. Therefore, the excellent class contains a very high number of

pixels. Therefore this operation applies a low sensitivity to a position.

$$\mu(x) = \prod_{i=1}^{i=n}(1 - \mu_i) \qquad (9)$$

- Fuzzy gamma (Eq. 10) – this operation represents the multiplication of the "fuzzy SUM" by the "fuzzy PRODUCT" to the power of gamma. The function becomes closer to the "fuzzy SUM" as gamma tends towards 1. On the contrary, it is closer to the "fuzzy product" when gamma tends to zero.

$$\mu(x) = (fuzzy\ SUM)^{\gamma} \times \\ \times (fuzzy\ PRODUCT)^{\gamma-1} \qquad (10)$$

where: γ – a parameter chosen in the interval 0 and 1. In this study, the value of the gamma operator (λ) is 0.9 (Parsian et al., 2021).

Validation procedures

To validate the flood susceptibility mapping models in the Wadi Assaka watershed, we used the locations of the historical inventories carried out within the study. The inventory of the flood-prone areas of the Draa and Guelmim watersheds was provided by the Hydraulic Watershed Agency of Draa Oued Noun (DONHBA). In addition to flood-prone areas, the visualization of high-resolution satellite images (0.41m) of the Geo-Eye-1 sensor as well as the field works was used to validate the results of our study. Therefore, this step allowed obtaining relevant information on 71 flooding sites, represented mainly by wadi beds, agricultural areas, road infrastructures, plains, and urbanized areas. On the other hand, 53 locations with a low risk of flooding were integrated. The ROC curve (Receiver operating characteristics) allows us to evaluate the performance of the models, and it is often used for binary classification problems (0 or 1). The ROC curve is showing the relationship between the true positive rate (TPR) and the false positive rate (FPR) (DeLong et al., 1988; Mas et al., 2013). For this study, the TPR describes the proportion of all flood locations correctly classified as flood occurrences, while the FPR shows the proportion of non-flooded points incorrectly classified as flood locations (Bouamrane et al., 2022; Falah et al., 2019; Vafakhah et al., 2020).

The flood susceptibility maps ROC curves were calculated using ArcGIS 10.5 software.

The mapping becomes more accurate as the curve approaches the upper left corner of the graph. Once the rate curves have been developed, the corresponding areas under the curve (AUC) are calculated. For an ideal model, AUC=1, and a random model, AUC=0.5. A model is usually considered to be good when the AUC value is greater than 0.7. A well-discriminating model should have an AUC between 0.87 and 0.9. A model with an AUC above 0.9 is excellent (Carter et al., 2016; Vafakhah et al., 2020; Vakhshoori & Zare, 2016).

RESULTS AND DISCUSSION

Final flood hazard maps

After preparing all the input factors. We applied the AHP method using Equation 3. The weighted overlay of the factors in raster format was performed using ArcGIS 10.5 (Figure 6). While, the application of fuzzy operators (OR, SUM, PRODUCT, AND, GAMMA 0.9) allows the generation of FLM-based flood susceptibility maps of the study area (Figure 6). Indeed, the visual analysis of the results obtained by the application of these methods on the selected factors showed that the three most relevant factors for the determination of flood risk are distance to rivers, flow accumulation, and elevation.

Evaluationg the performances and accuracies of the fuzzy methods

Flood susceptibility maps were generated based on fuzzy operators (OR, SUM, PRODUCT, AND, GAMMA 0.9) (Figure 5). Each flood susceptibility map was assigned to five intensity classes: very low, low, moderate, high, and very high; showing the percentages of occupied areas of each class for each model (Table 8). Fuzzy PRODUCT ranked a significant percentage of the study area as a very low susceptibility class (90.06%), while the highest susceptibility class represents only 0.8%. Next, fuzzy AND classified a large area (65.64%) in the very low susceptibility class, while, only 1.33% is a very high flood susceptibility class. Thereafter, fuzzy GAMMA, reveals the highest percentage of 38.08% as a very low susceptibility class, and the lowest percentage of 6.64% as a very high flood susceptibility class (Table 8). On the opposite, the highest flood
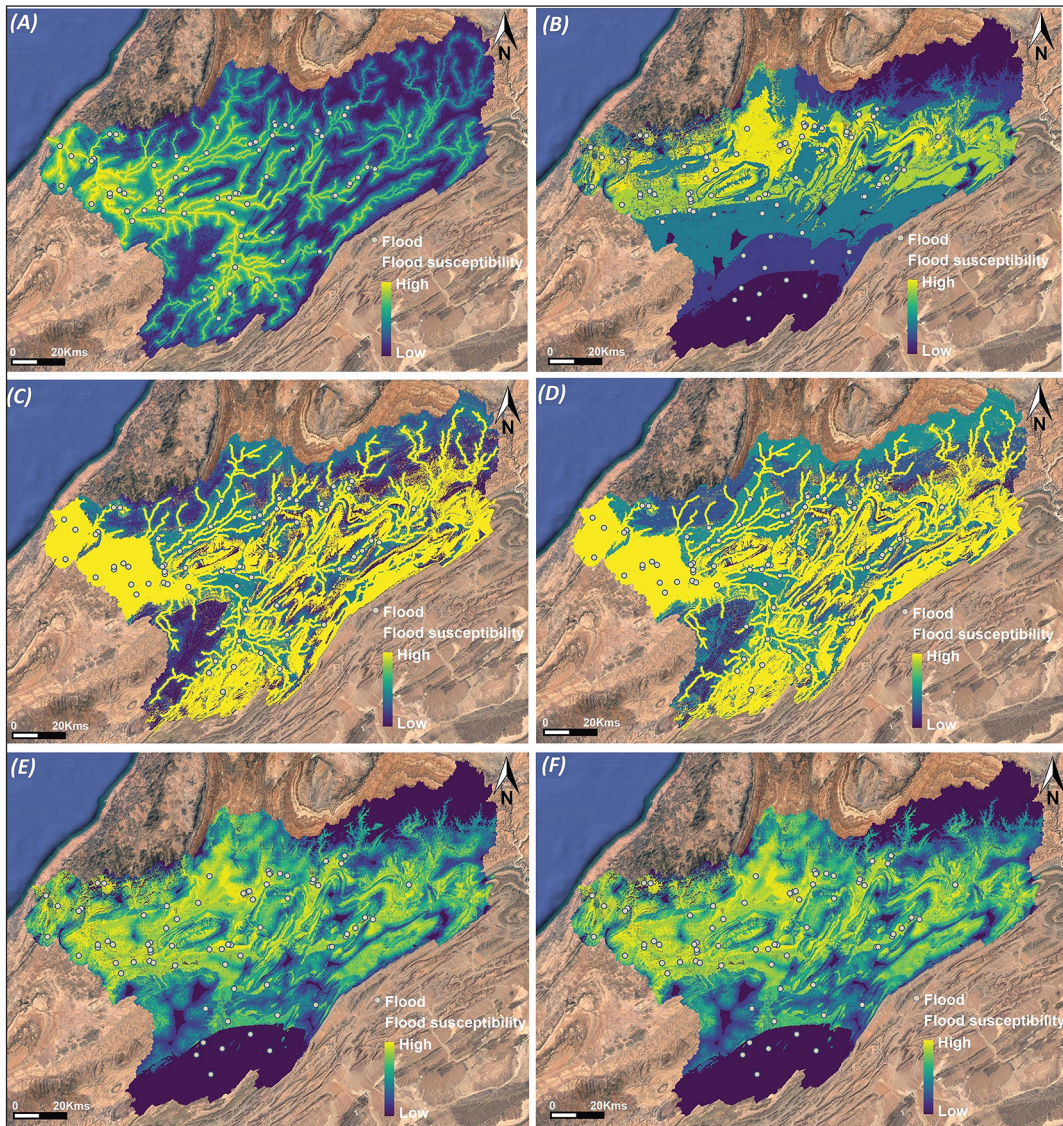
Figure 5. Flood susceptibility zonation maps derived from (a) AHP; (b) Fuzzy AND; (c) Fuzzy SUM; (d) Fuzzy OR; (e) Fuzzy Product; (f) Fuzzy Gamma 0.9 models

susceptibility classes were ranked as the largest area percentages with 64.42% and 39.23%, using OR and SUM operators, respectively. The smallest area percentage (0.7%) with very low flood susceptibility was obtained by the OR operator, followed by SUM with a percentage of a very low flood susceptibility area of 4.23% (Table 8).

Figure 6 shows the ROC curves of the fuzzy operators used in this study. Only the fuzzy SUM and fuzzy OR operators showed the best results, with AUC = 0.901 for the SUM operator and AUC = 0.896 for the fuzzy OR. The other operators showed less relevant results, with an AUC value = 0.710 for the fuzzy GAMMA 0.9 operator, and an AUC value = 0.708 for the fuzzy PRODUCT operator. Last is the fuzzy AND operator, which has the lowest percentage accuracy

(AUC = 0.668). In other words, the fuzzy SUM and fuzzy OR operators perform better than the other fuzzy operators (GAMMA 0.9, PRODUCT, and AND).

For effective flood susceptibility management in the study area, the fuzzy SUM and fuzzy OR models are the best. While the fuzzy GAMMA 0.9, fuzzy PRODUCT and fuzzy AND models are the least efficient. The low performance of these models can be due to their capacity for generalization and the way of manipulating the causal factors of the flood. Concerning the fuzzy GAMMA 0.9 and fuzzy PRODUCT models, they seem to under-generalize flood susceptibilities and only take into account the mean values of the conditioning factors. In addition, the Fuzzy AND model, gives the worst result, due to the

Table 8. Percentages of areas in each susceptibility class by using fuzzy logic models

Susceptibility classes	Fuzzy AND	Fuzzy PRODUCT	Fuzzy OR	Fuzzy SUM	Fuzzy Gamma 0.9
Very high	1.33	0.8	64.42	39.23	6.24
High	2.64	0.26	15.14	28.18	12.17
Medium	20.32	3.18	11.05	8.32	19.09
Low	10.07	5.7	8.69	15.04	24.42
Very low	65.64	90.06	0.7	9.23	38.08
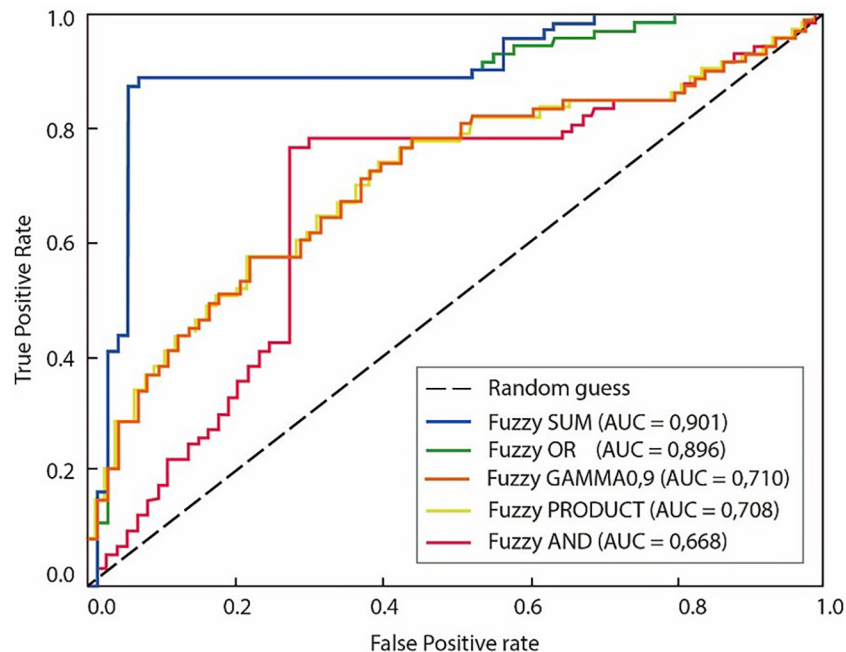
Figure 6. ROC curves calculated from the fuzzy logic model

inappropriate contribution of priorities between conditioning factors. For this model, the most relevant factors are rainfall and lithology. Nevertheless, it is interesting to note that fuzzy SUM and fuzzy OR operators remain the methods that are capable of providing useful information for monitoring, evaluating, and managing floods in the Assaka watershed.

Validation and comparison of the flood susceptibility maps using Fuzzy logic and AHP

From the visual interpretation (Figure 7), the maps simulated with both models show a fairly good agreement for the very sensitive areas, generally located downstream, towards the east of the watershed, and in the south. Compared to the analytical hierarchical process (AHP), the fuzzy logic method is more sensitive. Specific differences were distinguished, with some areas, such as the far northwest, being moderately sensitive according to the AHP

method, whereas they were identified as highly sensitive according to the fuzzy logic method (SUM). Thus, the floodplain to the west of the watershed is completely characterized as highly susceptible to flooding according to the fuzzy logic model. However, the AHP method considers a very high to high susceptibility in the vicinity of the Wadis (Figure 7).

In the Assaka watershed, the flood susceptibility maps created by the AHP and fuzzy logic methods were classified into five classes (very high, high, moderate, low, and very low) by applying natural break statistics (Akay, 2021). The flood maps created by both models were assessed using the GeoEye-1 satellite image (Figure 7). The obtained maps by the two methods are compared and validated by field observations and satellite images (Figure 7d). The number of points where the flood susceptibility was correctly assessed is 64 (90.01%) and 66 (92.29%) using the AHP and fuzzy logic models respectively.

In this way, we were able to determine the different vulnerable areas. Indeed, the AHP method showed that 8.4% (578 km²) of the study area has a very high susceptibility, 21.6% has a high risk (1483 km²), 30.5% has a moderate risk, 27.2% has a low risk and the remaining 12.13% has the lowest susceptibility. Nevertheless, Fuzzy Logic showed that 39.29% (2700 km²) of the study watershed is affected by very high flood susceptibility, 28.18% (1935 km²) has moderate susceptibility and the remaining 24.27% has low to very low susceptibility (Figure 8).

To quantitatively determine which technique is more efficient, receiver operating characteristics (ROC) curves were used (Figure 8). Compared to the AHP model, the ROC curve for fuzzy logic is closer to the upper left corner of the graph. The results obtained showed good accuracy for the AHP model (AUC=0.893) and a much slightly higher accuracy for the fuzzy logic model (AUC=0.901). Indeed, the fuzzy logic model reveals much less accurate results than the AHP method in identifying flood-susceptible areas. However, the AHP results are more compatible with several previous studies in the Assaka watershed (Bannari et al., 2018; Echogdali et al., 2022; Talha et al., 2019)

Fuzzy logic is a method that allows more flexible combinations of weighted maps without any prior classification; thus, its implementation is easy by using a GIS environment. However, this technique also has limitations when the experts' opinions are not too clear with uncertainty and subjectivity. Moreover, in several studies, the number of causal factors strongly influences the performance of the fuzzy logic model and in several cases, the fuzzy SUM operator is very sensitive, which makes this technique overestimate or underestimate the susceptibility (Akay, 2021; Bouamrane et al., 2022; Mudashiru et al., 2021; Vakhshoori & Zare, 2016).

AHP as well remains a widely used method to practice and doesn't require a large amount of information. In flood susceptibility mapping, this technique has given satisfactory results in many studies around the world (El Morjani et al., 2016;
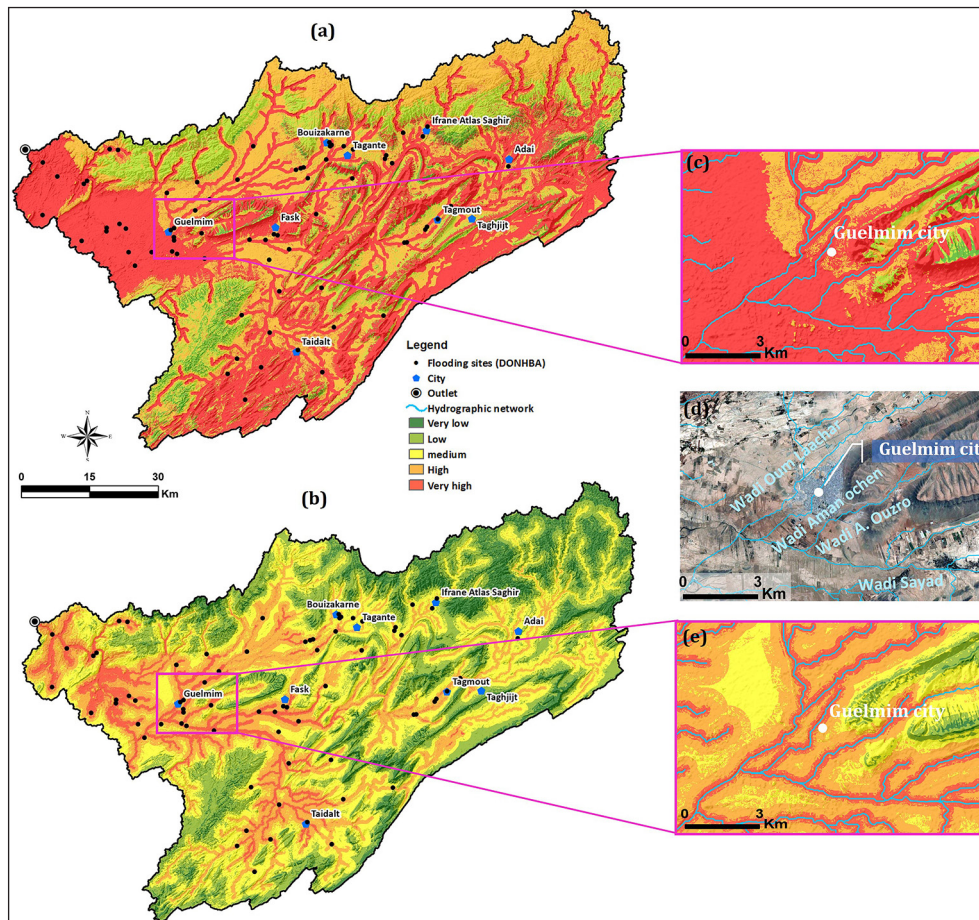
Figure 7. Flood susceptibility maps in the Assaka watershed using (a) Fuzzy SAM method and (b) AHP method and a zoomed view of the Guelmim urban center (c) Fuzzy SUM-derived map, (d) GeoEye-1 satellite image, and (e) AHP derived map

Kazakis et al., 2015; Wang et al., 2018). Nevertheless, the main weakness of the AHP is the pairwise comparison between the factors, which can give good scores for some criteria and bad scores for others. Hence, the modeling quality using the AHP is influenced by the expert's subjectivity (El Morjani, 2002; Mudashiru et al., 2021).

Numerous studies chose GAMMA-fuzzy logic in suitability analysis studies. As an example, (Parsian et al., 2021) used AHP to extract a weight for the fuzzified flood factor layers, then, a GAMMA operator in the other to generate a flood hazard map in the western part of Iran. While the present study demonstrated that a comparative analysis of the fuzzy operators is required to choose the optimum one. SUM-fuzzy logic generates more realistic results than GAMMA-fuzzy logic in our study area (Figure 5) as well as with a high AUC (90.1%).

In this context, a more detailed comparison focuses on the urbanized center of Guelmim. This latter is characterized by the largest population, which amounts to 118,318 inhabitants, and uncontrolled land use that makes it very vulnerable to flooding. In addition, this area represents a part of the floodplain that is affected by catastrophic floods caused by Wadi Oum Laachar, Wadi Aman Ocehn, Wadi Assif Ouzro, and Wadi Sayed. These are fed by several river systems from the Anti-Atlas, which generates exceptional floods. These Wadis join and constitute the Wadi Assaka. Indeed, the fuzzy logic model results rank this area as highly susceptible to flood. This technique considers principally all the runoff areas (even the secondary ones) as areas of high susceptibility to a flood (Figure 7c). However, the AHP method gives priority to areas closer to the main river systems, flow, and elevation; this allows preferential mapping of areas that are very high to highly exposed to flood risk (Figure 7e).

In this study, both techniques practically show that susceptibility increases with increasing proximity to the main Wadis, which are responsible for several catastrophic floods, which killed at least 28 people during the period of 20-24 November 2014. Indeed, during this period, these Wadis (Oum Laachar, Aman Ocehn, Assif Ouzro, and Sayed) overflowed the two bridges located in the urban perimeter of the city of Guelmim, on the National Road No. 12 connecting Guelmim to Sidi Ifni and on the National Road No. 1 (Figure 7d). These two roads were cut off during this period. In addition, several irrigated perimeters were also affected, such as the Oum Aghanim perimeter, the Rouissate perimeter, the Oum Laachar perimeter, and the Khadroua perimeter, which occupy a useful agricultural area of 15,000 hectares. Thus, during this period, cuts in water, electricity, and telecommunication networks; undermined roads, and houses were invaded and destroyed (Figure 9).

Implications of this study

Our study consists in mapping the flood risks in the Assaka watershed, using a multi-factorial assessment approach (AHP and FLM), carried out in a GIS environment. Seven important factors conditioning the occurrence of floods were introduced in the models, namely: flow accumulation, elevation, slope, land use, distance to the river, lithology, and rainfall. Therefore, all priority areas, which present a very high risk, must be considered to better plan the management and restoration of Wadis. This will reduce the damage and losses caused by floods in the study area. Hereby it can be said that both approaches are
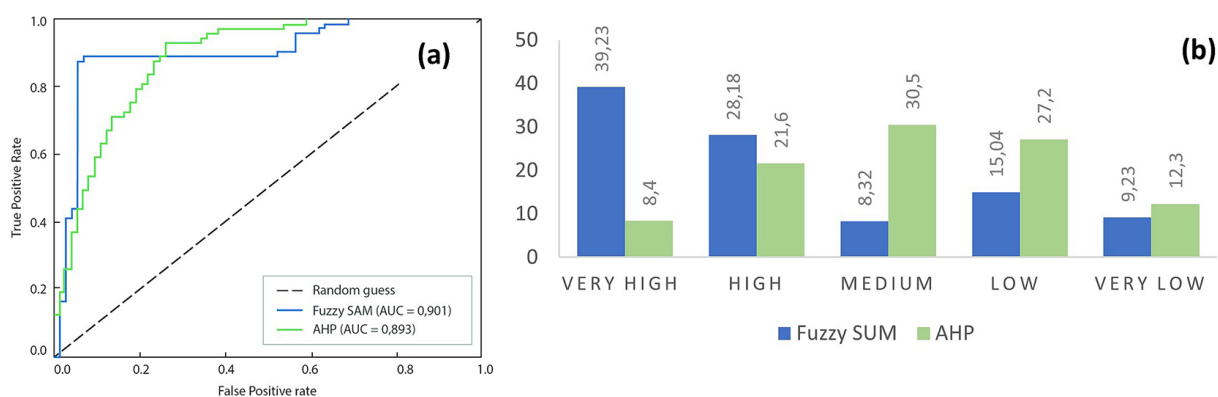
Figure 8. (a) AUC values of AHP and Fuzzy logic models; (b) percentages of flood susceptibility area by class, using fuzzy logic and AHP method

Figure 9. Photographs showing the damage caused by the floods in the Assaka watershed's urbanized areas; (a) Flooded zone at the center of Guelmim City; (b) Collapsing at the Bridge on the RN1; (c) Raising of the water level in the wadi Oum Laachar during a flood period; (d) Destruction of roadways in the Wadis neighborhoods

equally effective in other regions. Indeed, the results of this paper can be used to:

- the improvement of the hierarchy of flood highly susceptible regions, and identification areas that urgently require hydraulic modeling studies, immediate rehabilitation (minor beds controlling and improvement of the sewerage system), and hydraulic developments (construction of dykes, dams, bridges, and protective walls...) against flood events;
- the elaboration of urbanization suitability maps, which allows appropriate planning of urban and rural living areas, agricultural areas, transport infrastructures, and industrial areas;
- equipping the main Wadis of the catchment area (upstream, middle, and downstream) with an early warning system of floods, by implanting hydrometeorological stations, capable of following flows and water heights in a regular way. Thus, the development of a web mapping platform with public access, for the updated location of flood histories;
- further research into the relevant reasons for variations in performance between the models used. In addition, try other more advanced techniques such as artificial intelligence methods that can improve the spatial mapping of floods in the Assakawatershed or other regions.

CONCLUSIONS

The fundamental objective of our study is to present a practical and simple methodology to recognize the degree of flood susceptibility in the Assaka watershed. Indeed, the AHP method and the fuzzy logic modeling integrated with GIS, have proven to be efficient and provide better results necessary for the efficient monitoring and management of flood risks. The integration of AHP and several fuzzy logic models in the present study allowed us to obtain convenient information about the effect of several relevant factors for an accurate flood susceptibility mapping. Moreover, based on the obtained results main conclusions of our study can be summarized as follows. The observation of close correlations between flood-prone areas and spatial distributions of conditioning factors, including distance to rivers, flow accumulation, and elevation. Only the fuzzy SUM and fuzzy OR operators showed the best results for the fuzzy logic method, with AUC = 0.901 for the SUM operator and AUC = 0.896 for the fuzzy OR. The AHP method (AUC = 0.893) and the SUM operator of the fuzzy logic method (AUC = 0.901) can be considered a complementary technique, very powerful and capable of providing reliable information for the monitoring and management of floods in

the Assakawatershed. Initiate further studies to further explore the reasons for variations in performance between the models used. In addition, we plan to test the methods of artificial intelligence (Data-driven algorithms), which can improve the assessment of flood susceptibility. This work is considered as part of the first steps towards the enhancement of a geospatial dataset, supplementing other thematic maps (hydrogeology, pedology, lineaments, roads, social factors, etc.) to reconstitute useful support for any further investigations in our study area context.

Acknowledgments

REFERENCES

1. Aide, T., Szönyi, M., Saidi, A.D. 2015. Morocco floods of 2014: what we can learn from Guelmim and Sidi Ifni. Zurich Insurance Group Ltd.: Zurichh, Switzerland.

2. Akay, H. 2021. Flood hazards susceptibility mapping using statistical, fuzzy logic, and MCDM methods. Soft Computing, 25(14), 9325–9346.

3. Amouch, S., Akhssas, A., Bahi, L., Bennouna, R. 2020. Characterisation of recent and future climatic trends in the region of Guelmim (Morocco). E3S Web of Conferences, 150, 03021.

4. Andrade, T., Rodrigues, H., Bourguignon, M., Cordeiro, G. 2015. The exponentiated generalized Gumbel distribution. Revista Colombiana de Estadística, 38(1), 123–143.

5. Apollonio, C., Balacco, G., Novelli, A., Tarantino, E., Piccinni, A.F. 2016. Land use change impact on flooding areas: The case study of Cervaro Basin (Italy). Sustainability, 8(10), 996.

6. Argaz, A., Ouahman, B., Darkaoui, A., Bikhtar, H., Ayouch, E., Lazaar, R. 2019. Flood hazard mapping using remote sensing and GIS Tools: a case study of souss watershed. Journal of Materials and Environmental Sciences, 10, 170–181.

7. Atbir, H., Charif, A., Malek, H.A., Akdim, B., Louazani, M. 2021. Étude Géomorphologique des héritages quaternaires de la région de Lakhsass-Guelmim (versant sud de l'Anti-Atlas occidental, Maroc).

8. Bannari, A., Kadhem, G., El-Battay, A., Hameid, N. 2018. Comparison of SRTM-V4. 1 and ASTER-V2. 1 for accurate topographic attributes and hydrologic indices extraction in flooded areas. Journal of Earth Science and Engineering, 8, 8–30.

9. Barkey, R., Malamassam, D., Mukhlisa, A., Nursaputra, M. 2020. Land use planning for floods mitigation in Kelara Watershed, South Sulawesi Province, Indonesia. IOP Conference Series: Earth and Environmental Science, 575, 012132.

10. Bouamrane, A., Derdous, O., Dahri, N., Tachi, S.-E., Boutebba, K., Bouziane, M.T. 2022. A comparison of the analytical hierarchy process and the fuzzy logic approach for flood susceptibility mapping in a semi-arid ungauged basin (Biskra basin: Algeria). International Journal of River Basin Management, 20(2), 203–213.

11. Carter, J.V., Pan, J., Rai, S.N., Galandiuk, S. 2016. ROC-ing along: Evaluation and interpretation of receiver operating characteristic curves. Surgery, 159(6), 1638–1645.

12. Çavur, M., Duzgun, H., Kemeç, S., Demirkan, D. 2019. Land use and land cover classification of Sentinel 2-A: St Petersburg case study. The International Archives of Photogrammetry, Remote Sensing and Spatial Information Sciences, 42, 13–16.

13. Chen, F.-W., Liu, C.-W. 2012. Estimation of the spatial rainfall distribution using inverse distance weighting (IDW) in the middle of Taiwan. Paddy and Water Environment, 10(3), 209–222.

14. Costache, R., Pham, Q.B., Sharifi, E., Linh, N.T.T., Abba, S.I., Vojtek, M., Vojteková, J., Nhi, P.T.T., & Khoi, D.N. 2019. Flash-flood susceptibility assessment using multi-criteria decision making and machine learning supported by remote sensing and GIS techniques. Remote Sensing, 12(1), 106.

15. D'Avignon, G.R., Sauvageau, M. 1996. L'aide multicritère à la décision: un cas d'intégration de critères techniques, économiques et environnementaux à Hydro-Québec. RAIRO-Operations Research, 30(3), 317–332.

16. Dash, P., Sar, J. 2020. Identification and validation of potential flood hazard area using GIS-based multi-criteria analysis and satellite data-derived water index. Journal of Flood Risk Management, 13(3), e12620.

17. DeLong, E.R., DeLong, D.M., & Clarke-Pearson, D.L. 1988. Comparing the areas under two or more correlated receiver operating characteristic curves: a nonparametric approach. Biometrics, 44(3), 837-845.

18. Demir, V., Kisi, O. 2016. Flood hazard mapping by using geographic information system and hydraulic model: Mert River, Samsun, Turkey. Advances in Meteorology, 2016, 4891015.

19. Echogdali, F., Boutaleb, S., Jauregui, J., & Elmouden, A. 2018. Cartography of flooding hazard in semi-arid climate: the case of Tata Valley (South-East of Morocco). Journal of Geography & Natural Disasters, 8(214), 2167–0587.1000214.

20. Echogdali, F., Boutaleb, S., Kpan, R., Ouchchen, M., Id-Belqas, M., Dadi, B., Ikirri, M., Abioui, M. 2022. Flood hazard and susceptibility assessment in a semi-arid environment: A case study of Seyad basin, south of Morocco. Journal of African Earth Sciences, 196, 104709.

21. El Mahmouhi, N., El Wartiti, M., Wissem, S.A., Kemmou, S., El Bahi, S. 2016. Utilisation des systèmes d'information géographiques et des modèles hydrologiques pour l'extraction des caractéristiques physiques du bassin versant d'Assaka (Guelmim, sud du Maroc)[The use of geographic information system for the extraction of physical characteristics of assaka watershed: sub-basins of sayed and oum laachar wadis (southern Morocco)]. International Journal of Innovation and Applied Studies, 16(2), 370–377.

22. El Morjani, Z., Seif Ennasr, M., Elmouden, A., Idbraim, S., Bouaakaz, B., Saad, A. 2016. Flood hazard mapping and modeling using GIS applied to the Souss river watershed. In: Choukr-Allah R. et al. (Eds), The Souss-Massa river basin, Morocco (The handbook of environmental chemistry 53). Springer, Switzerland, pp. 57–93.

23. El Morjani, Z.E.A. 2002. Conception d'un système d'information à référence spatiale pour la gestion environnementale: application à la sélection de sites potentiels de stockage de déchets ménagers et industriels en région semi-aride (Souss, Maroc). PhD Dissertation, University of Geneva].

24. Falah, F., Rahmati, O., Rostami, M., Ahmadisharaf, E., Daliakopoulos, I.N., Pourghasemi, H. R. 2019. Artificial neural networks for flood susceptibility mapping in data-scarce urban areas. In Spatial modeling in GIS and R for Earth and Environmental Sciences. Elsevier, 323–336.

25. Farhadi, H., Najafzadeh, M. 2021. Flood risk mapping by remote sensing data and random forest technique. Water, 13(21), 3115.

26. Goovaerts, P. 2000. Geostatistical approaches for incorporating elevation into the spatial interpolation of rainfall. Journal of hydrology, 228(1–2), 113–129.

27. Grillakis, M.G., Polykretis, C., Manoudakis, S., Seiradakis, K.D., Alexakis, D.D. 2020. A quantile mapping method to fill in discontinued daily precipitation time series. Water, 12(8), 2304.

28. Gumbel, E. 1957. Méthodes graphiques pour l'analyse des débits de crues. Revue de statistique appliquée, 5(2), 77–89.

29. Ha, H., Bui, Q.D., Nguyen, H.D., Pham, B.T., Lai, T.D., Luu, C. 2023. A practical approach to flood hazard, vulnerability, and risk assessing and mapping for Quang Binh province, Vietnam. Environment, Development and Sustainability, 25(2), 1101–1130.

30. Hajaj, S., El Harti, A., Jellouli, A., Pour, A.B., Himyari, S.M., Hamzaoui, A., Bensalah, M.K., Benaouiss, N., Hashim, M. 2023. HyMap imagery for copper and manganese prospecting in the east of Ameln valley shear zone (Kerdous inlier, western Anti-Atlas, Morocco). Journal of Spatial Science, 1–22.

31. Hammami, S., Zouhri, L., Souissi, D., Souei, A., Zghibi, A., Marzougui, A., Dlala, M. 2019. Application of the GIS based multi-criteria decision analysis and analytical hierarchy process (AHP) in the flood susceptibility mapping (Tunisia). Arabian Journal of Geosciences, 12, 653.

32. Hu, Q., Li, Z., Wang, L., Huang, Y., Wang, Y., Li, L. 2019. Rainfall spatial estimations: A review from spatial interpolation to multi-source data merging. Water, 11(3), 579.

33. Ikirri, M., Faik, F., Echogdali, F.Z., Antunes, I.M.H.R., Abioui, M., Abdelrahman, K., Fnais, M.S., Wanaim, A., Id-Belqas, M., Boutaleb, S. 2022. Flood hazard index application in arid catchments: Case of the taguenit wadi watershed, Lakhssas, Morocco. Land, 11(8), 1178.

34. Jari, A., El Mostafa Bachaoui, A.J., El Harti, A., Khaddari, A., El Jazouli, A. 2022. Use of GIS, remote sensing and analytical hierarchy process for groundwater potential assessment in an arid region – A case study. Ecological Engineering and Environmental Technology, 23(5), 234–255.

35. Karmaoui, A., Messouli, M., Khebiza, Y.M., Ifaadassan, I. 2014. Environmental vulnerability to climate change and anthropogenic impacts in dryland,(pilot study: Middle Draa Valley, South Morocco). Journal of Earth Science & Climatic Change, (S11), 002.

36. Kazakis, N., Kougias, I., Patsialis, T. 2015. Assessment of flood hazard areas at a regional scale using an index-based approach and Analytical Hierarchy Process: Application in Rhodope–Evros region, Greece. Science of the Total Environment, 538, 555–563.

37. Khaddari, A., Bouziani, M., Moussa, K., Sammar, C., Chakiri, S., Hadi, H. E., Jari, A., Titafi, A. 2022. Evaluation of Precipitation Spatial Interpolation Techniques using GIS for Better Prevention of Extreme Events: Case of the Assaka Watershed (Southern Morocco). Eco. Env. & Cons, 28, 1–10.

38. Khosravi, K., Pourghasemi, H.R., Chapi, K., Bahri, M. 2016. Flash flood susceptibility analysis and its mapping using different bivariate models in Iran: a comparison between Shannon's entropy, statistical index, and weighting factor models. Environmental Monitoring and Assessment, 188, 656.

39. Komi, K., Neal, J., Trigg, M.A., Diekkrüger, B. 2017. Modelling of flood hazard extent in data

sparse areas: a case study of the Oti River basin, West Africa. Journal of Hydrology: Regional Studies, 10, 122–132.

40. Kouassi, A., Nassa, R., Yao, K., Kouame, K., Biemi, J. 2018. Modélisation statistique des pluies maximales annuelles dans le District d'Abidjan (Sud de la Côte d'Ivoire). Revue des sciences de l'eau/Journal of Water Science, 31(2), 147–160.

41. Li, Q., Zhou, J., Cai, J., Zhou, J. 2018. The environmental study on flash flood risk zonation based on trapezoidal fuzzy number and grey clustering. Ekoloji, 27(106), 2015–2025.

42. Malekinezhad, H., Sepehri, M., Pham, Q.B., Hosseini, S.Z., Meshram, S.G., Vojtek, M., Vojteková, J. 2021. Application of entropy weighting method for urban flood hazard mapping. Acta geophysica, 69(3), 841–854.

43. Marengo, J.A., Camarinha, P.I., Alves, L.M., Diniz, F., Betts, R.A. 2021. Extreme rainfall and hydro-geo-meteorological disaster risk in 1.5, 2.0, and 4.0° C global warming scenarios: an analysis for Brazil. Frontiers in Climate, 3, 610433.

44. Mas, J.-F., Filho, B.S., Pontius Jr, R.G., Gutiérrez, M.F., Rodrigues, H. 2013. A suite of tools for ROC analysis of spatial models. ISPRS International Journal of Geo-Information, 2(3), 869–887.

45. Mathieu, J., Weisrock, A., Wengler, L., Brochier, J.E., Even, G., Fontugne, M., Mercier, N., Ouammou, A., Senegas, F., Valladas, H. 2004. Holocene deposits in the lower section of the Assaka wadi, South Morocco: Preliminary results. Quaternaire, 15(1–2), 207–218.

46. Mirari, S. 2022. Développement du tourisme durable à travers l'approche du Marketing Territorial dans la province de Guelmim-Maroc. Espace Géographique et Société Marocaine, 57, 93–115.

47. Mirari, S., Benmlih, A. 2018. The Sustainable Development of Oued Noun Oases through the Integration in the Biosphere Reserve Oasis of Southern Morocco. Int. J. Sci. Res, 7, 1211–1218.

48. Mohamed, M.M., Elmahdy, S.I. 2017. Fuzzy logic and multi-criteria methods for groundwater potentiality mapping at Al Fo'ah area, the United Arab Emirates (UAE): an integrated approach. Geocarto international, 32(10), 1120–1138.

49. Morjani, Z. 2011. Methodology Document for the WHO e-atlas of Disaster Risk. Volume 1. Exposure to Natural Hazards Version 2.0 Flood Hazard Modelling. In: Taroudant Poly-Disciplinary Faculty of the Ibn Zohr University of Agadir.

50. Msaddek, M., Kimbowa, G., El Garouani, A. 2020. Hydrological modeling of upper OumErRabia Basin (Morocco), comparative study of the event-based and continuous-process HEC-HMS model methods. Computational Water, Energy, and Environmental Engineering, 9(4), 159.

51. Mudashiru, R.B., Sabtu, N., Abustan, I., Balogun, W. 2021. Flood hazard mapping methods: A review. Journal of hydrology, 603, 126846.

52. Nandalal, H., Ratnayake, U. 2011. Flood risk analysis using fuzzy models. Journal of Flood Risk Management, 4(2), 128–139.

53. Nguyen, P., Thorstensen, A., Sorooshian, S., Hsu, K., Agha Kouchak, A., Sanders, B., Koren, V., Cui, Z., Smith, M. 2016. A high resolution coupled hydrologic–hydraulic model (HiResFlood-UCI) for flash flood modeling. Journal of hydrology, 541, 401–420.

54. Nwazelibe, V.E., Unigwe, C.O., Egbueri, J.C. 2023. Testing the performances of different fuzzy overlay methods in GIS-based landslide susceptibility mapping of Udi Province, SE Nigeria. Catena, 220, 106654.

55. Odabas, M.S., Leelaruban, N., Simsek, H., Padmanabhan, G. 2014. Quantifying impact of droughts on barley yield in North Dakota, USA using multiple linear regression and artificial neural network. Neural Network World, 24(4), 343.

56. Onen, F., Bagatur, T. 2017. Prediction of flood frequency factor for Gumbel distribution using regression and GEP model. Arabian Journal for Science and Engineering, 42(9), 3895–3906.

57. Ongdas, N., Akiyanova, F., Karakulov, Y., Muratbayeva, A., Zinabdin, N. 2020. Application of HEC-RAS (2D) for flood hazard maps generation for Yesil (Ishim) river in Kazakhstan. Water, 12(10), 2672.

58. Parsian, S., Amani, M., Moghimi, A., Ghorbanian, A., Mahdavi, S. 2021. Flood hazard mapping using fuzzy logic, analytical hierarchy process, and multi-source geospatial datasets. Remote Sensing, 13(23), 4761.

59. Phiri, D., Simwanda, M., Salekin, S., Nyirenda, V.R., Murayama, Y., Ranagalage, M. 2020. Sentinel-2 data for land cover/use mapping: a review. Remote Sensing, 12(14), 2291.

60. Pourghasemi, H.R., Beheshtirad, M., Pradhan, B. 2016. A comparative assessment of prediction capabilities of modified analytical hierarchy process (M-AHP) and Mamdani fuzzy logic models using Netcad-GIS for forest fire susceptibility mapping. Geomatics, Natural Hazards and Risk, 7(2), 861–885.

61. Roy, B., Bouyssou, D. 1993. Aide multicritère à la décision: méthodes et cas. Economica Paris.

62. Saaty, T. L. 1977. A scaling method for priorities in hierarchical structures. Journal of mathematical psychology, 15(3), 234–281.

63. Saaty, T.L. 1990. How to make a decision: the analytic hierarchy process. European journal of operational research, 48(1), 9–26.

64. Saaty, T.L., Vargas, L.G. 2012. The seven pillars of the analytic hierarchy process. In Models, methods, concepts & applications of the analytic hierarchy process. International Series in Operations Research & Management Science, vol. 175, Springer, Boston.

65. Sadeghi, B., Khalajmasoumi, M. 2015. A futuristic review for evaluation of geothermal potentials using fuzzy logic and binary index overlay in GIS environment. Renewable and Sustainable Energy Reviews, 43, 818–831.

66. Sahana, M., Patel, P.P. 2019. A comparison of frequency ratio and fuzzy logic models for flood susceptibility assessment of the lower Kosi River Basin in India. Environmental Earth Sciences, 78, 289.

67. Samanta, R.K., Bhunia, G.S., Shit, P.K., Pourghasemi, H.R. 2018. Flood susceptibility mapping using geospatial frequency ratio technique: a case study of Subarnarekha River Basin, India. Modeling Earth Systems and Environment, 4, 395–408.

68. Schwarz, I., Kuleshov, Y. 2022. Flood Vulnerability Assessment and Mapping: A Case Study for Australia's Hawkesbury-Nepean Catchment. Remote Sensing, 14(19), 4894.

69. Shafapour Tehrany, M., Kumar, L., Neamah Jebur, M., Shabani, F. 2019. Evaluating the application of the statistical index method in flood susceptibility mapping and its comparison with frequency ratio and logistic regression methods. Geomatics, Natural Hazards and Risk, 10(1), 79–101.

70. Siahkamari, S., Haghizadeh, A., Zeinivand, H., Tahmasebipour, N., Rahmati, O. 2018. Spatial prediction of flood-susceptible areas using frequency ratio and maximum entropy models. Geocarto international, 33(9), 927–941.

71. Siler, W., Ying, H. 1989. Fuzzy control theory: The linear case. Fuzzy sets and systems, 33(3), 275–290.

72. Sonmez, O., Bizimana, H. 2020. Flood hazard risk evaluation using fuzzy logic and weightage-based combination methods in geographic information system. Scientia Iranica, 27(2), 517–528.

73. Soulaimani, A., Bouabdelli, M. 2005. Le Plateau de Lakhssas (Anti-Atlas occidental, Maroc): Un graben fini-précambrien réactivé à l'hercynien. Ann. Soc. Géol. Nord, 2(2), 177–184.

74. Soulaimani, A., Ouanaimi, H. 2011. Anti-Atlas et Haut Atlas, circuit occidental. Nouveaux guides géologiques et miniers du Maroc, 3, 9–72.

75. Tabari, H. 2020. Climate change impact on flood and extreme precipitation increases with water availability. Scientific reports, 10(1), 13768.

76. Tah, J.H., Carr, V. 2000. A proposal for construction project risk assessment using fuzzy logic. Construction Management & Economics, 18(4), 491–500.

77. Talha, S., Maanan, M., Atika, H., Rhinane, H. 2019. Prediction of flash flood susceptibility using fuzzy analytical hierarchy process (Fahp) algorithms and Gis: a study case of guelmim region In Southwestern of Morocco. The International Archives of Photogrammetry, Remote Sensing and Spatial Information Sciences, 42, 407–414.

78. Tanguy, M. 2012. Cartographie du risque d'inondation en milieu urbain adaptée à la gestion de crise: Analyse préliminaire. INRS-Eau, Terre et Environnement: Quebec City, QC, Canada

79. Theilen-Willige, B., Charif, A., El Ouahidi, A., Chaibi, M., Ougougdal, M.A., AitMalek, H. 2015. Flash floods in the Guelmim area/Southwest Morocco–use of remote sensing and GIS-tools for the detection of flooding-prone areas. Geosciences, 5(2), 203–221.

80. Tie, A.G.B., Konan, B., Brou, Y.T., Issiaka, S., Fadika, V., Srohourou, B. 2007. Estimation des pluies exceptionnelles journalières en zone tropicale: cas de la Côte d'Ivoire par comparaison des lois Lognormale et de Gumbel. Hydrological sciences journal, 52(1), 49–67.

81. Vafakhah, M., Mohammad Hasani Loor, S., Pourghasemi, H., Katebikord, A. 2020. Comparing performance of random forest and adaptive neuro-fuzzy inference system data mining models for flood susceptibility mapping. Arabian Journal of Geosciences, 13, 417.

82. Vakhshoori, V., Zare, M. 2016. Landslide susceptibility mapping by comparing weight of evidence, fuzzy logic, and frequency ratio methods. Geomatics, Natural Hazards and Risk, 7(5), 1731–1752.

83. Vignesh, K., Anandakumar, I., Ranjan, R., Borah, D. 2021. Flood vulnerability assessment using an integrated approach of multi-criteria decision-making model and geospatial techniques. Modeling Earth Systems and Environment, 7(2), 767–781.

84. Wang, Y., Fang, Z., Hong, H., Peng, L. 2020. Flood susceptibility mapping using convolutional neural network frameworks. Journal of hydrology, 582, 124482.

85. Wang, Y., Hong, H., Chen, W., Li, S., Pamučar, D., Gigović, L., Drobnjak, S., Tien Bui, D., Duan, H. 2018. A hybrid GIS multi-criteria decision-making method for flood susceptibility mapping at Shangyou, China. Remote Sensing, 11(1), 62.

86. Werren, G., Reynard, E., Lane, S.N., Balin, D. 2016. Flood hazard assessment and mapping in semi-arid piedmont areas: a case study in Beni Mellal, Morocco. Natural Hazards, 81, 481–511.

87. Yurdakul, M. 2004. AHP as a strategic decision-making tool to justify machine tool selection. Journal of Materials Processing Technology, 146(3), 365–376.

88. Zadeh, L.A. 1965. Fuzzy sets. Information and control, 8(3), 338–353.

89. Zorn, M. 2018. Natural disasters and less developed countries. In: Pelc, S., Koderman, M. (Eds.), Nature, Tourism and Ethnicity as Drivers of (De)Marginalization. Perspectives on Geographical Marginality, vol. 3. Springer, Cham. .